Clinics and Research in Hepatology and Gastroenterology (2019) 43, 669—681

Available online at ScienceDirect www.sciencedirect.com

Elsevier Masson France EM|consulte www.em-consulte.com/en

ORIGINAL ARTICLE

Cavitation-induced release of liposomal chemotherapy in orthotopic murine pancreatic cancer models: A feasibility study

Marine Camus[a,b,*], Ariane Vienne[a], Jean-Louis Mestas[c], Carlos Pratico[a,d], Carole Nicco[a,d], Christiane Chereau[a,d], Jean-Martial Marie[c], Alexei Moussatov[c], Gilles Renault[a,d], Frederic Batteux[a,d], Cyril Lafon[c], Frederic Prat[a,d]

[a] *Inserm U1066, institut Cochin, 75014 Paris, France*
[b] *Sorbonne université, AP—HP, hôpital Saint Antoine, 75012 Paris, France*
[c] *LabTAU, INSERM, Centre Léon Bérard, Université-Lyon 1, Lyon, 69003, Lyon, France*
[d] *Université Paris Descartes, hôpital Cochin, AP—HP, 75014, Paris, France*

Available online 26 April 2019

KEYWORDS
Ultrasound;
Drug delivery;
Liposome;
Cavitation;
Chemoresistance;
Pancreatic cancer

Summary Targeted and triggered release of liposomal drug using ultrasound (US) induced cavitation represents a promising treatment modality to increase the therapeutic-toxicity ratio of encapsulated chemotherapy.
Objectives: To study the feasibility and efficacy of a combination of focused US and liposomal doxorubicin (US-L-DOX) release in orthotopic murine models of pancreatic cancer.
Material and methods: A confocal US setup was developed to generate US inertial cavitation delivery in a controlled and reproducible manner and designed for two distinct murine orthotopic pancreatic cancer models. Controlled cavitation at 1 MHz was applied within the tumors after L-DOX injection according to a preliminary pharmacokinetic study.
Results: In vitro studies confirmed that L-DOX was cytostatic. In vivo pharmacokinetic study showed L-DOX peak tumor accumulation at 48h. Feasibility of L-DOX injection and US delivery was demonstrated in both murine models. In a nude mouse model, at W9 after implantation (W5 after treatment), US-L-DOX group (median [IQR] 51.43 mm^3 [35.1—871.95]) exhibited significantly lower tumor volumes than the sham group (216.28 [96.12—1202.92]), the US group (359.44 [131.48—1649.25]), and the L-DOX group (255.94 [84.09—943.72]), and a trend, although not statistically significant, to a lower volume than Gemcitabine group (90.48 [42.14—367.78]).

* Corresponding author at: Endoscopy Unit, Cochin Hospital, 27, rue du Faubourg-St-Jacques, 75014 Paris, France
E-mail address: marine.camus@aphp.fr (M. Camus).

https://doi.org/10.1016/j.clinre.2019.02.015

Conclusion: This study demonstrates that inertial cavitation can be generated to increase the therapeutic effect of drug-carrying liposomes accumulated in the tumor. This approach is potentially an important step towards a therapeutic application of cavitation-induced drug delivery in pancreatic cancer.

Introduction

Pancreatic ductal adenocarcinoma (PDAC), one of the most dreadful malignancies and the fourth commonest cause of cancer death in the Western world, [1] is rapidly increasing in incidence [2]. The overall 5-year survival rate is less than 5%, and has not significantly improved over the past three decades [3]. Surgical resection is the only curative option, but even in specialized centers, the 5-year survival rate of ''curatively'' operated patients remains under 30% [4,5]. Moreover, surgical resection is not feasible in 80% of the patients because of early local and metastatic spread of the disease [6]. Chemotherapy is the standard of care for locally advanced and metastatic pancreatic cancer [7]. Although intensified cytotoxic combinations, particularly gemcitabine plus nab-paclitaxel and the folinic acid, fluorouracil, irinotecan, oxaliplatin (FOLFIRINOX) protocol have recently provided some convincing improvement in metastatic PDAC when compared with previous standard gemcitabine regimen, significant therapeutic breakthroughs remain out of sight [8,9]. Since chemoresistance and abundant desmoplastic stroma of PDAC are major barriers to efficient chemotherapy [10,11] and dose limitation is necessary to avoid dangerous cytotoxicity, there is a need for more efficient delivery of therapeutic drugs at the disease target while limiting toxicity to healthy tissue.

Heat and ultrasound, among others, have been suggested as promising actuators of physically-triggered release of encapsulated drugs. Ultrasound (US) in particular, has the potential to trigger release in a well-defined volume of tissue by fine-focusing the US beam and creating local cavitation, thus increasing the therapeutic-toxicity ratio of encapsulated drugs in a specific target tissue [12]. As discussed later in this article, improving therapeutic effects by mimicking cavitation using microbubble-based ultrasound contrast agents (MBUCA) has been proposed, [13—17] but using sonosensitive liposomal chemotherapy instead of MBUCA+standard chemotherapy is another innovative and promising pathway [18]. We recently proved the safety for adjacent healthy tissue of inertial cavitation combined with doxorubicin administration in the absence of MBUCA in a mouse model of breast cancer, [19] as well as the increased therapeutic effect of inertial cavitation combined with doxorubicin-loaded liposomes in a AT2 Dunning rat ectopic tumor model [20,21].

Nevertheless, to our knowledge, there has been no in vivo study evaluating the efficacy of focused ultrasound in combination with sono-sensitive liposomes loaded with chemotherapy to improve the chemotherapeutic efficacy in orthotopic murine models of PDAC [22].

The aims of this study were to investigate the feasibility of using a focused US device for cavitation-induced drug release using a sonosensitive liposomal drug carrier, to assess the potential therapeutic benefit of such a treatment in orthotopic murine models of PDAC, and to determine possible issues raised by this approach.

Materials and methods

All experiments were performed in accordance with the European convention for the protection of vertebrate animals used for experimental and other scientific purposes. All animal experiments were approved by an independent ethics committee (*Comité d'Ethique en matière d'Expérimentation Animale*, *University Paris 5 René Descartes, CEEA 34*) and in agreement with the national ethics rules for animal experimentation [23].

A flow chart to clarified animals experiments are available on S4 Fig.

Rat tumor model

The model used in this study was described by Hotz in 2001 [24]. Five-week-old male Lewis rats (LEW/CrlBR) weighing 100 to 150 g were obtained from Charles River Laboratories (Wilmington, MA, U.S.A.). The animals were housed in microisolator cages with autoclaved bedding, food, and water. The rats were maintained on a daily 12-hour light/12-hour dark cycle. Rats were operated on at an age varying from 7 to 10 weeks (weight 140-315g) for tumor implantation of DSL6A/C1 cells. The rat PDAC cell line DSL-6A/C1 was purchased from the American Type Culture Collection (Rockville, MD, U.S.A.), and cultured in Waymouth's MB 752/1 medium (Gibco, Grand Island, NY, U.S.A.). The cell-culture medium was supplemented with 10% heat inactivated fetal bovine serum (FBS; Gibco), 1% penicillin G-streptomycin and 1% ciprofloxacin. Cells were incubated at 37 °C in moisturized air with 5% CO2. The medium was replaced twice weekly, and cells were maintained by serial passaging after trypsinization with 0.1% trypsin. 10^7 Cells were injected subcutaneously into each flank of donor rats in a total volume of 0.2 mL. The rats were killed by a lethal dose of pentobarbital (50 mg, i.p.) after the subcutaneous tumors had reached a size of 15 to 20 mm in the largest diameter. Necrotic tissues were cut away, and the remaining healthy tumor tissues were harvested under strict aseptic conditions and minced into fragments of 4.5 mm^3. Tumor fragments were maintained in culture cell medium until implantation. Under anesthesia, the abdomen of tumor

recipient rats was sterilised with alcohol, an incision was created through the left upper abdominal pararectal line and peritoneum, the spleen with the tail of the pancreas was gently exteriorised and 2 tumor pieces were implanted into microsurgically prepared tissue pockets within the pancreatic parenchyma, so that the tumor tissue was completely surrounded by pancreatic parenchyma without requiring the use of sutures. The pancreas was then returned into the peritoneal cavity, and the abdominal wall and the skin were closed in 2 layers using 4—0 surgical suture.

For subcutaneous cell injection and all ultrasound procedures, rats were anaesthetised by inhalation of 2.5% Isofluorane. For orthotopic implantation, the animals were anaesthetised by pentobarbital (40mg/kg/i.p) after conditioning by Isofluorane inhalation. The rats were killed by a lethal dose of pentobarbital (50 mg, i.p.) at the end of the experiments or if one of the following events occurred: bulky tumor mass with visible tumor size > 3 cm; formation of ascites with visible abdominal distension; or cachexia associated with a significant clinical deterioration of the animal.

Nude mice tumor model

Similarly to the rat model, we used an orthotopic PDAC model in nude mice. 4-week-old female nude mice (NMRI-Foxn1nu/nu) weighing 20 g were obtained from Janvier Labs (Le Genest-Saint-Isle, France). The animals were operated on at an age varying from 6 to 8 weeks for tumor implantation of MiaPaca2 cells. The human ductal pancreatic adenocarcinoma cell line MiaPaca2 was purchased from the American Type Culture Collection (Rockville, MD, U.S.A.), and cultured in DMEM Glutamax medium (Gibco, Grand Island, NY, U.S.A.). The cell-culture medium was supplemented with 10% heat inactivated fetal bovine serum (FBS; Gibco), 1% penicillin G-streptomycin and 1% ciprofloxacin. 5×10^6 Cells were injected subcutaneously into each flank of donor mice in a total volume of 0.2 mL. The donor mice were killed by a lethal dose of pentobarbital (50 mg, i.p.) after the subcutaneous tumors had reached a size of 15 to 20 mm in the largest diameter. The implantation of orthotopic tumor in receiver nude mice followed the same experimental and surgical steps as the Lewis rat. However only one tumor fragment was implanted in mice, using calibrated 1mm-diameter pieces.

Histologic analysis

The primary orthotopic tumors were removed and saved for histologic analysis. Tumor tissues were fixed in 10% buffered formalin and paraffin-embedded. Hematoxylin and eosin (H&E) staining was performed on paraffin-embedded tumour tissues with a slice thickness of 6 μm.

Method of Ultrasound Imaging and Tumor Measurement and Correlation with Macroscopic Findings

Ultrasound imaging was performed by two trained operators in an animal-dedicated imaging platform on a high-resolution ultrasound Vevo 770 (Visualsonics, Toronto, Canada) with a 40MHz probe (RMV704), under general anaesthesia with isofluorane (2.5%, 2 mL/min). Tumors were detected as circular lesions discretely hypoechogenic compared to the surrounding pancreatic parenchyma. Tumor volume was derived from the 2 largest perpendicular diameters by the following approximation: ultrasound volume = (length $\times$ width^2)/2. When there was more than one individualised tumor, each tumor was measured separately and added to count a total per animal tumor volume. The reliability of the detection and measurement of the orthotopically-developed tumors was assessed in 16 rats. At sacrifice time-point, real-time determination of tumor volume was performed by ultrasound followed by an autopsy. The 3 larger perpendicular diameters of the primary orthotopic tumor were measured with callipers, and the volume was calculated using the following formula: volume = length $\times$ width $\times$ depth/2 as described previously by Hotz et al. [24]. The correlation coefficient could then be calculated between tumor volume and ultrasound tumor measurements.

In vitro Efficacy of Gemcitabine (GEM), Doxorubicin (DOX) and Liposomal Doxorubicin (L-DOX)

The effects of liposomal DOX (L-DOX) were assessed in vitro on DSL6A/C1 cell line in comparison to free Doxorubicin (DOX), (DOXORUBICIN DAKOTA PHARM® 10mg, Sanofi-Aventis) and Gemcitabine (GEMZAR®, 200mg, Lilly France), a standard chemotherapy of PDAC. Sono-sensitive liposomes loaded with doxorubicin (L-DOX) were obtained under a venture with Epitarget company and prepared as described previously [20,25]. DOX concentration was 1 mg/ml with an encapsulation efficiency of DOX greater than 90%. Liposome diameter was measured by photon correlation spectroscopy with a Malvern Zetasizer Nano ZS (Malvern Instruments, Malvern, UK). The liposomes showed a mean hydrodynamic diameter of 85 ± 2 nm, with polydispersity index < 0.1, indicating a narrow size distribution. The small size of these liposomes has been shown to be useful both in terms of in vivo stability by way of limiting opsonisation, and in the enhancement of extravasation and tumor uptake [26]. These specific liposomes have demonstrated in vitro sonosensitivity properties [27] justifying their use *in vivo* in combination with ultrasound.

To assess the cytostatic effect of chemotherapy drugs, a proliferation experiment with incorporation of tritiated thymidine at 48 hours was performed, along with Crystal violet staining to evaluate the cytotoxicity. The experiments were performed in triplicate 4 times for each drug at increasing concentrations (L-DOX: 0,05 to 5 μM; DOX: 0,3 to 20 μM; Gemcitabine: 0.1 nM to 2.5 μM). The DSL6A/C1 cell line was cultured has described above.

Biodistribution/pharmacokinetic studies

In order to determine the peak time of liposome accumulation in tissue, a biodistribution/pharmacokinetics study was undertaken on 2 cohorts of 15 animals (pooled results). The animals included in this experiment were

carriers of pancreatic tumors implanted for 6 weeks and ultrasonically detectable. Doxorubicin-loaded sonosensitive liposomes were used.

At 6 weeks after pancreatic tumor graft, liposomes were injected i.p. at a dose of 4 mg L-DOX per kg body weight. Doses were based on clinically used L-DOX (Doxil™/Caelyx™) that has physicochemical properties similar to those of the sonosentive liposomes used in this study.

At selected timepoints (12, 24, 36, 48, and 72h) post injection ($n = 3$ per timepoint), rats were euthanized by intraperitoneal injection of dolethal (1 ml per animal). Liver, spleen, kidney, and tumor tissues were excised, weighed, snap frozen in liquid nitrogen and subsequently stored at −20 °C.Thawed tissues were weighed and digested with acidified ethanol (0.3 M HCl in 50% ethanol) at a final 1:10 dilution ratio (1 g tissue sample to 9 ml acidified ethanol). The mixture was homogenized (Polytron, Fisher Scientific, Illkirch, France) until a tissue homogenate was obtained, which was incubated for 24 hours at 4 °C in the dark. After incubation, triplicates of tissue homogenate (2 mL each) were centrifuged at 10,000 g for 20 min at 4 °C to separate cell debris. Clear supernatants were stored at −20 °C until fluorescence measurements were performed. The property of spontaneous fluorescence of DOX to 596 nm after excitation at 492 nm light was used for measuring the fluorescence in different organs. The actual L-DOX content was determined based on relevant L-DOX calibration curves obtained from similar animals without injection of L-DOX. The results of two successive experiments were pooled.

Therapy study

Tumor sonication apparatus

A US device previously developed for subcutaneous tumors [21] had to be modified for application in orthotopic pancreatic tumors (Fig. 1) [21,28]. Modifications were undertaken to take into consideration new treatment modalities (positioning of the transducers, use of degassed water and real-time detection of tumors by US-scan). A device was designed to have the animal in prone position in order to facilitate tumor identification and targeting. This device consisted of two concave power transducers, positioned at 110° and immersed in degassed water, thermostatically maintained at 37 °C, allowing transmission of ultrasound into the abdomen without loss of energy or formation of microbubbles on the skin surface. Water was degassed using a suction pump with a multi-perforated outlet [29]. A low frequency US probe (10 MHz Vermon® plateform Orchéo XQ, SonoScanner®) was coupled to a detection system positioned 25 mm from the confocality of ultrasonic beams, in order to target the tumor and observe cavitation in real time. A support system was designed to keep the animal under isofluorane anesthesia, mobilize the animal relative to the axis of the transducers, identify and target the tumor.

The successive processing steps of a therapeutic US session were as follows:

- anesthesia, and animal hair removal;
- tumor detection with ultrasound 40 MHz and localization of the best firing window (skin marking);
- positioning the transducers below the animal abdomen;
- ultrasound shot, monitored by 10 MHz probe.

Therapeutic US parameters applied were derived from a previous study on subcutaneous tumors, and modified for the treatment of more deeply-seated tumors. The parameters applied for each models are described in Table 1. The setup was completed using a Wattmeter which allowed to fix the command for the sonication system. The number of US shots was tailored to the volume area as estimated intraoperatively by US scan. The pancreas was irradiated spot by spot until the whole section visible on the ultrasound imaging was treated. The impacts were separated by 2mm in the 3 directions. At each irradiation, the forward and reverse power were checked and no devation from the setting was observed. The duration of each shot was 2 seconds.

Rat treatment and follow-up

The outline of the therapy study is summarized in Table 1. Six groups of all animals were studied : sham, US alone, DOX, L-DOX, US + DOX, US + L-DOX.All rats received i.p. injected L-DOX (4 mg/kg) or free DOX (4 mg/kg) at week 4 after pancreatic tumor graft, if the tumor was more than 10 mm^3 in estimated volume and had increased in volume between to 2 US-scans at week 2 and 3. US treatment was applied at 48 hours post-injection, corresponding to peak L-DOX content in tumor tissue. The animals were then followed with ultrasound measurement of tumor size at 1, 2 and 3 weeks after treatment and were sacrificed at 7 weeks, with macroscopic tumor measurement and sampling for pathology.

Mice treatment and follow-up

The outline of the therapy study is also summarized in Table 1. Two successive series of thirty nude mice were implanted, pooled and divided in five groups for further treatment: sham US alone, L-DOX, Gemcitabine, US + L-DOX. All mice received i.p. injections of liposomal L-DOX (8 mg/kg) or Gemcitabine (100 mg/kg). Drugs were administered at 4 weeks after pancreatic tumor graft. US treatment was applied at 48 hours post-injection. The animals were then followed with ultrasound measurement of tumor size at 1, 2, 3, 4 et 5 weeks after treatment and were sacrificed 9 weeks after implantation, with macroscopic tumor measurement and sampling for pathology.

Statistical Analysis

Data are presented as mean ± SD or median [Interquartile range IQR]. Mann-Whitney test was used for pharmacokinetic results. Volume correlation (ultrasound volume vs. volume at sacrifice) was measured using Pearson correlation coefficient. $P < 0.05$ was statistically significant.

One series of rats followed by two pooled series of nude mice were analyzed. As the distribution of tumor volume in nude mice was log-normal (Kolmogorov test $p_{value} = 0.15$ at W3) data have been transformed using the logarithm function for the different populations to obtain a normal dis-

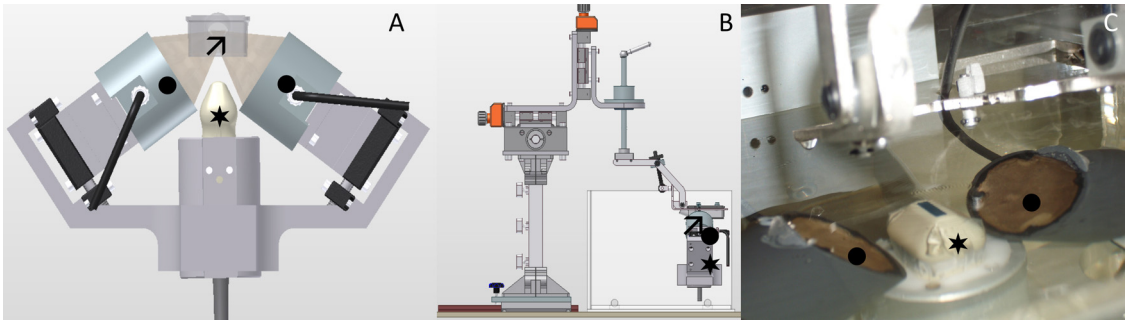

Figure 1 US delivery system. The mice is placed on prone position to allow tumor detection and to facilitate treatment by two-focused transducers. Three differents views. A Front view of the device. B. Lateral view of the device. C. Top view of the device (*US probe to detect and target tumor, ✶ support system for animal, and ● two concave power transducers).

Table 1 Experimental groups of two murine models receiving different treatments.

Model of orthotopic pancreatic cancer	Groups	Number of animals	Drugs received	US treatment	Ultrasound parameters
Immunocompetent rat	1	6	Saline/Vehicule	-	Average electrical power: 6W;
Lewis model	2	5	Saline/Vehicule	+	Ultrasound frequency: 1.1MHz;
DSL6A cell line	3	5	DOX (4 mg/kg)	-	Pulse Repetition
	4	5	DOX (4 mg/kg)	+	Frequency (PRF): PRF=200Hz;
	5	5	L-DOX (4 mg/kg)	-	Duty cycle (effective ultrasound
	6	6	L-DOX (4 mg/kg)	+	emission rate) DC=0.77%
Subtotal	6	32			
Nude mice model	1	8	Saline/Vehicule	-	Average electrical power: 5.85W;
MiaPaca2 cell line	2	9	Saline/Vehicule	+	Ultrasound frequency: 1.1 MHz;
	3	8	GEM (100 mg/kg)	-	PRF = 250 Hz;
	4	9	L-DOX (8 mg/kg)	-	DC = 1%
	5	9	L-DOX (8 mg/kg)	+	
Subtotal	5	43			

DOX: doxorubicin ; GEM : gemcitabine ; L-DOX: liposomal-Doxorubicin.

tribution (at W3 mean ± SD = 2.78 ± 1.15; Shapiro-Wilk test p_{value} = 0.71) and to allow further analysis.

To study the tumor growth week by week for each group, tumor volume was standardized for each series data at the randomization week. Then linear regression was used to analyse and compare the evolution of tumor volume between groups. There was a significant difference when confidence intervals did not overlap ($P < 0.05$).

Statistical analyses were performed under Graphpad Prism® (GraphPad Software, Inc., La Jolla, California, USA) and JMP (SAS Institute Inc., Cary, NC, USA).

Results

Ultrasound tumor measurement and correlation with macroscopic findings

Tumor ultrasound detection was always feasible within 6 to 10 minutes per animal, with good tolerance in both rats and mice (no animal death during US scans) (Fig. 2). Pancreatic tumors appeared as nodular images hypoechoic relative to the rest of the pancreas, close to the spleen. A nodular image on US scan corresponded histologically to a pancreatic ductal adenocarcinoma (Fig. 2). Tumor volumes estimated from US scans and those measured macroscopically with calipers were well correlated ($P < 0.0001$) (S1 Fig).

In vitro Efficacy of Gemcitabine (GEM), Doxorubicin (DOX) and Liposomal Doxorubicin (L-DOX)

The pooled results of experiments for cytostatic and cytotoxic effects are presented in Fig. 3. L-DOX decreased the proliferation of tumor cells (DSL6A/C1 cell line). L-DOX had a cytostatic effect but no significant antiproliferative effect (IC50 was not reach), whereas DOX and GEM had both cytostatic and cytotoxic effect.

In vivo biodistribution/pharmacokinetic study and determination of timespan between L-DOX injection and therapeutic US

Blood clearance kinetics of L-DOX and peak L-DOX tumor accumulation were determined to identify the optimal time-point for US treatment, as shown in Fig. 4. Pharmacokinetics in tumors and healthy pancreas revealed different profiles (Fig. 4A). A significant accumulation and retention of L-DOX

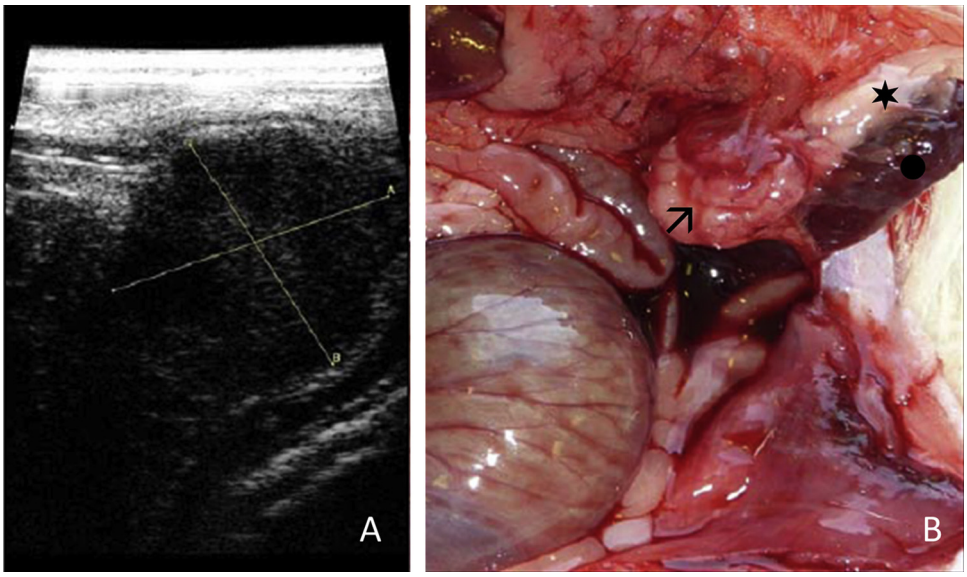

Figure 2 Example of PDAC tumor obtained in our murin models. A. US scanning: pancreatic tumor seen as a circular hypoechogenic lesion-image obtained with high-resolution ultrasound Vevo770 (Visualsonics) with a 40 MHz probe (RMV 704). B. macroscopic examination: at sacrifice, verification that the tumor grew in the pancreas, (*healthy pancreas, ✶ pancreatic tumor, and ● and spleen).

was observed in tumors 48h after injection, whereas the concentration of the drug in the healthy pancreas rapidly tended to zero ($P = 0.04$, Mann—Whitney test). Liposomes had a peak concentration at 36 hours after injection in the spleen, liver, and kidney and decreased at 48 hours, with very small residual concentrations in the liver and kidney at the same timepoint (Fig. 4B and Fig. S5). Based on these data it was decided to undertake US treatment 48 hours after liposome injection.

Outcome of ultrasound therapy

Tumor sonication process

The US delivery system is presented in Fig. 1. Upon triggering power, the ultrasound image was disrupted by pulses and blurred by cavitation microbubbles. At the end of a treatment session, a hyperechoic spot was visible in the treated area corresponding macroscopically to an area of necrosis (Fig. 5). This system allowed for a satisfactory location of tumors and the creation of cavitation with a good tolerance in all of the animals. The discrete size of the focal spot (2 mm in diameter) allowed for switching the transducer from one spot to the next so as to cover the whole tumor volume as estimated on US scan.

Outcomes in rats

Forty-three Lewis rats were implanted (with an implantation success rate of 74% (32/43). The 32 rats were distributed into 6 groups: sham (6 rats), US alone (5 rats), DOX (5 rats), L-DOX (5 rats), US + DOX (5 rats), US + L-DOX (6 rats). The weight of rats at baseline (treatment day, 4 weeks after implantation) ranged between 196 and 302 g (237 ± 24 g) and average tumor volume at the same timepoint was not different between groups, ranging from 163.4 to 191 mm^3 ($P > 0.05$, Table 2). Of the 16 animals undergoing ultrasound therapy, 6 had skin petechiae after treatment, especially in the case of tumors developed closest to the skin. The evolution of tumor volume after treatment is shown in Fig. 6A, with no significant difference between groups. Two rats had peritoneal carcinomatosis in the control group.

Since we observed heterogenous tumor growth profiles in Lewis rats, we studied the natural history of the Lewis Rat model in a series of 60 implanted, but untreated rats and found that amongst all animals with visible tumors (median volume 14.19 [0—9621] mm^3) at W4 ($n = 34/60$), only 15/60 (25%) were still growing at W6. A threshold of 80 mm^3 at W4 was found to be associated with subsequent tumour growth — 87% (13/15) of the tumors bigger than 80 mm^3 at W4 still growing at W6 (S2 Fig).

In consideration of these previously unreported natural history findings, there was an observable trend for decreased tumor growth in US alone, US+DOX and US+L-DOX groups compared to controls, when we considered only animals with tumors > 80 mm^3 at W4, but these results, with much smaller samples, lacked power to attain statistical significance (Fig. 6B).

Outcomes in Mice

Two successive series of 30 nude mice were implanted and subsequently pooled after confirming that volume distributions were not different at three weeks (Wilcoxon's test: $p_{value} = 0.21$). Forty-three mice (71.6%, 43/60) had successful tumor implant at W3. Two mice were excluded from the analysis due to rapid tumor regression (control group), leaving 41 mice available for therapy. The mean (±SD) estimated tumor volume at 3 weeks (W3) was 32.33 ± 50.16 mm^3 (Quantiles(mm^3) •25%: 7.27; •50%: 14.72; •75%: 35.00). and

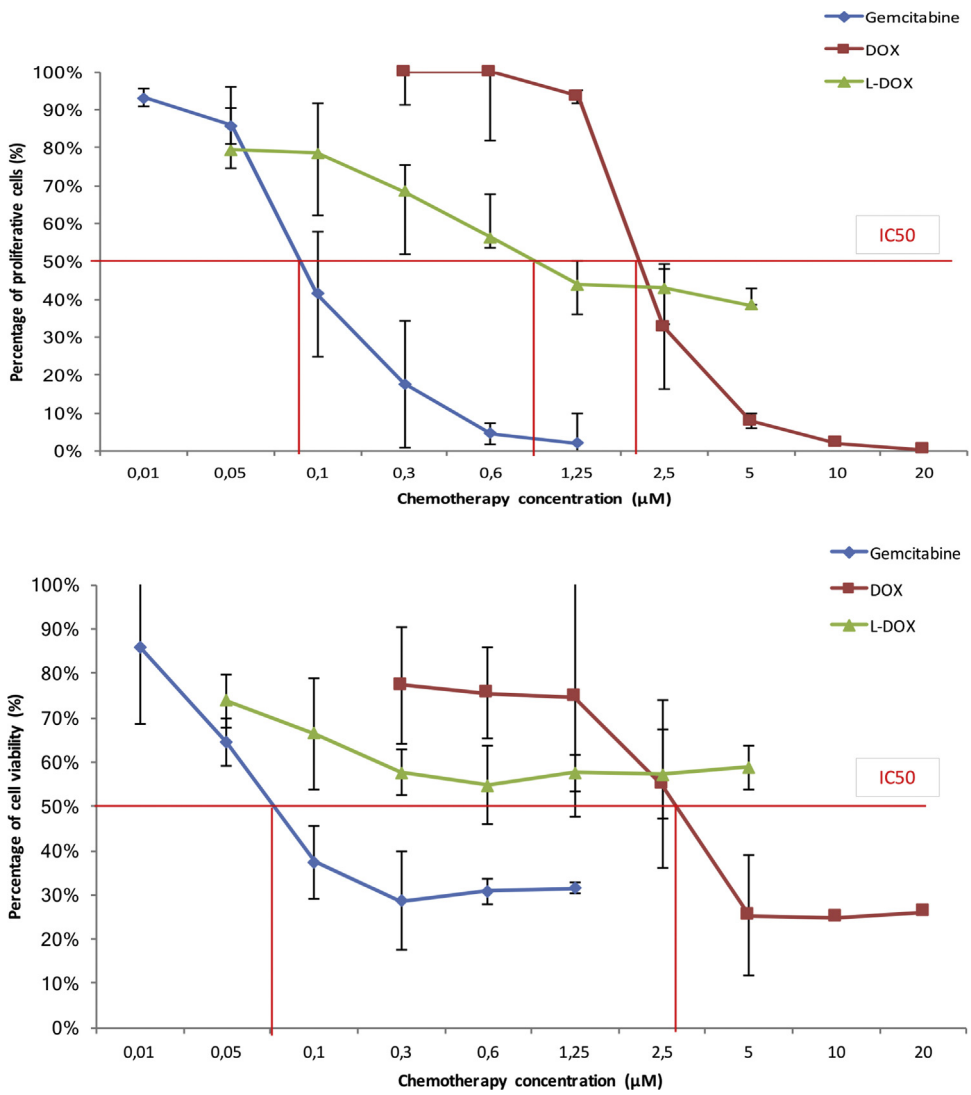

Figure 3 In vitro efficacy of Gemcitabine (GEM), Doxorubicin (DOX) and liposomal Doxorubicin (L-DOX). Results for cytostatic (Fig. 3A) and cytotoxic effects (Fig. 3B).

Table 2 Tumor volumes at treatment time (orthotopic PDAC immunocompetent rat model).

Groups	Number of animals	Drugs received	US treatment	Tumor volume (mm^3) at treatment time - week 4 Mean ± SD
1	6	Saline/Vehicule	-	163.4 ± 101
2	5	Saline/Vehicule	+	191.00 ± 92
3	5	DOX (4 mg/kg)	-	167.25 ± 67
4	5	DOX (4 mg/kg)	+	165.25 ± 120
5	5	L-DOX (4 mg/kg)	-	188.56 ± 78
6	6	L-DOX (4 mg/kg)	+	172.87 ± 93

DOX: doxorubicin; L-DOX: liposomal-doxorubicin.

similar between groups ($P > 0.05$, Table 3). Mice were allocated to five groups for treatment: sham (7 mice), US alone (9 mice), L-DOX (8 mice), Gemcitabine (8 mice), US + L-DOX (9 mice). Correlation between ultrasound tumor volumes and macroscopic tumor volumes at sacrifice in mice are shown in S3 Fig. Overall results of mice treatments are presented in Fig. 7. At W9 after implantation (five weeks after treatment), US-L-DOX group (median [IQR] 51.43 mm^3 [35.1—871.95]) exhibited significantly lower tumor volumes than the sham group (216.28 [96.12—1202.92]), the US group (359.44 [131.48—1649.25]), and the L-DOX group (255.94 [84.09—943.72]), and a trend, although not statistically significant, to a lower volume than Gemcitabine group (90.48 [42.14—367.78]).

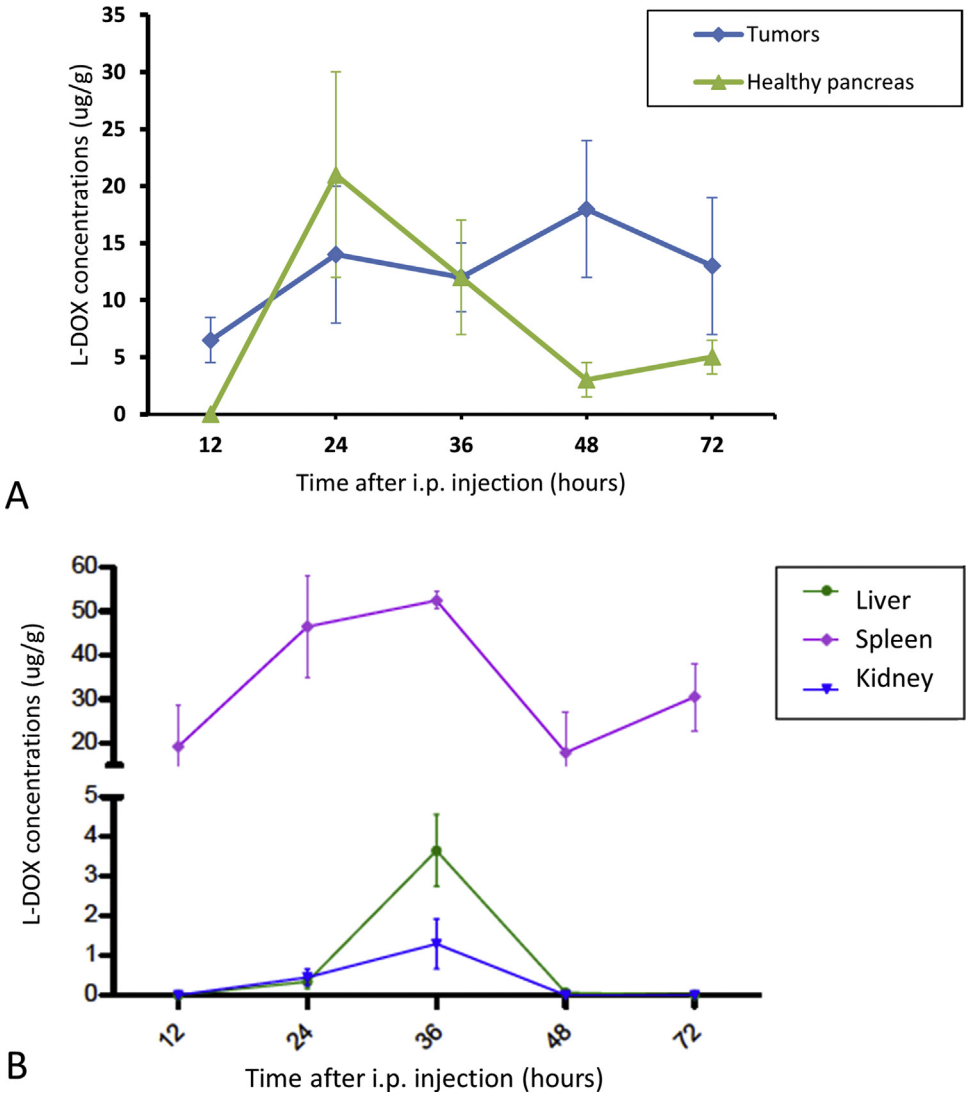

Figure 4 In vivo biodistribution/pharmacokinetic study of L-DOX in the pancreas, liver, kidneys and spleen of immunocompetent Lewis rat (*n*=30).

Table 3 Tumor volumes at treatment time (orthotopic PDAC nude mouse model).

Groups	Number of animals	Drugs received	US treatment	Tumor volume (mm^3) at randomization before treatment	
				Mean ± SD	Median (IQR)
1	8	Saline/Vehicule	-	46.77 ± 18.46	11.62 (3.77—34.24)
2	9	Saline/Vehicule	+	29.15 ± 17.40	9.06 (5.62—38.92)
3	8	GEM (100 mg/kg)	-	27.19 ± 17.40	15.71 (7.94—30.36)
4	9	L-DOX (8 mg/kg)	-	31.28 ± 18.46	20.58 (10.16—42.94)
5	9	L-DOX (8 mg/kg)	+	28.76 ± 17.4	17.96 (9.42—50.18)

DOX: doxorubicin; GEM: gemcitabine; L-DOX: liposomal-doxorubicin.

Discussion

This study demonstrates for the first time the feasibility and potential efficacy of a treatment combining ultrasonic cavitation and chemotherapy-loaded sonosensitive liposomes in deep intra-abdominal orthotopic PDAC models, using an original confocal ultrasound delivery device.

These results show that ultrasonic cavitation can be created in an orthotopic PDAC model using a dedicated US setup with real time assessment of cavitation. The treat-

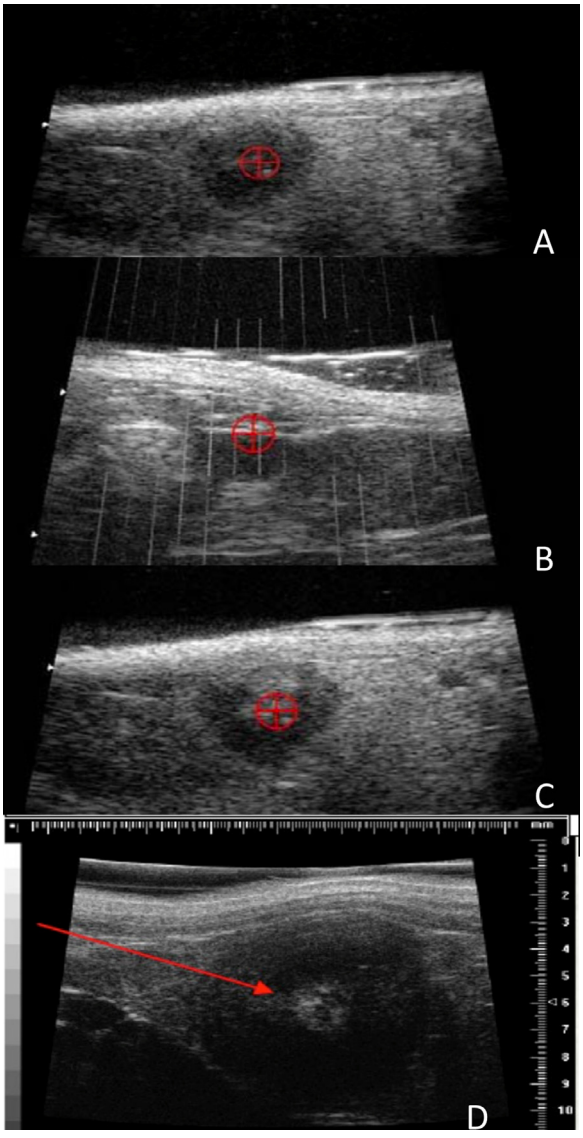

Figure 5 Tumor sonication process. A. Tumor detection with ultrasound and localization of the best firing window. B. Ultrasound application. C and D. Hyperechoic appearance of the treated area in the hypoechoic tumor).

ment was deemed feasible in all animals with no major side effects, which is consistent with previously published results [19]. The combination of two crossing beams is an efficient method to selectively create cavitation at the focal point without damage to adjacent tissues. Our setup with ultrasound imaging monitoring (10 MHz probe) also made it easy to visualize a tumor area that has just been treated in the sonicated field, thereby strongly suggesting that cavitation had actually occurred in the targeted volume (Fig. 5).

Encapsulation of chemotherapeutic agents into liposomes has been proven to reduce healthy tissue exposure to drugs en route to the tumor, thereby potentially reducing systemic side-effects. In previous pharmacokinetic experiments on L-DOX, we confirmed the occurrence of the liposome-associated enhanced permeability and retention (EPR) effect [30] with liposomes heavily accumulated in the tumor, but not in the normal tissue 48h after injection. The development of such drug delivery vehicles has to confront two conflicting challenges: the need for stable non-leaking particles in the general circulation, and the need for drug release at the diseased site [31] A PEGylated liposomal formulation of doxorubicin (Doxil® or Caelyx®) is now used routinely to treat metastatic breast cancer, advanced ovarian cancer, and Kaposi's sarcoma [32]. The therapeutic benefit of liposomal doxorubicin (L-DOX) over conventional doxorubicin (DOX) treatment is, however, mainly related to reduced cardio-toxicity, more than to improved antitumor efficacy. Uptake of liposomal drugs in cancer tissue is in itself not sufficient enough to ensure drug bioavailability and therapeutic action. US has been suggested as a promising treatment modality to improve the therapeutic-toxicity ratio of encapsulated drugs on a specific target tissue [33,34]. US offers the additional benefit of increasing cell permeability, via the so-called sonoporation process, thus providing a two-fold effect: drug-carrier disruption and increased intracellular drug uptake [35].

Our study brings preliminary efficacy data, particularly in the nude mouse model, with the US-L-DOX group exhibiting significantly slower tumor-growth after 9 weeks of follow-up than control, and US-alone groups. To our knowledge, this is the first in vivo study combining sonosensitive liposome with US exposition in pancreatic cancer. Earlier studies have shown in vitro and in vivo mostly that microbubble-based ultrasound contrast agents (MBUCA)-based sonoporation is a viable technique to improve drug delivery and therapeutic efficacy in various cell lines derived from glioma, [37] and melanoma, [39] as well as prostate, [38], pharyngeal, [36] and pancreatic cancers [40]. Sonoporation has also been recently used to open up the blood brain barrier in a safe and well tolerated manner in a pilot clinical trial of glioblastoma patients [41]. Based on these clinical and preclinical results, an open label phase I, single center, safety evaluation study in ten PDAC patients was conducted by combining a contrast-enhanced ultrasound agent (SonoVue®, Bracco Imaging Scandinavia AB, Oslo, Norway) and gemcitabine under sonication. Combination treated patients ($n = 10$) tolerated an increased number of gemcitabine cycles compared with historical controls ($n = 63$ patients (average of 8.3 ± 6.0 cycles, vs. 13.8 ± 5.6 cycles, $P = 0.008$, unpaired t-test) without any additional toxicity or increased frequency of side effects [13]. However this comparison concerned a very small number of patients with historical controls, and there has been neither an assessment of the optimal US regimen, nor any demonstration of improved bioavailability after microbubble and US application. Most studies in the literature combined low-pressure waves, in the MPa range, with MBUCA to facilitate the initiation of cavitation [14—17]. Similar cavitation activity can be obtained without MBUCA by using much higher negative-pressure levels [42,43]. One advantage of this method is to get rid of the need for MBUCA, which have a very short and elusive presence in the peritumoral microcirculation, since the high negative pressure generates cavitation bubbles in the vicinity of blood vessels and in poorly vascularized tissues that cannot be reached by standard MBUCA, which is most likely in PDAC. The presence of a dense stroma that separates cancer cells from the blood vessels is a major factor of reduced tissue permeability [44,45]. This dense stroma has also been shown to cause high interstitial

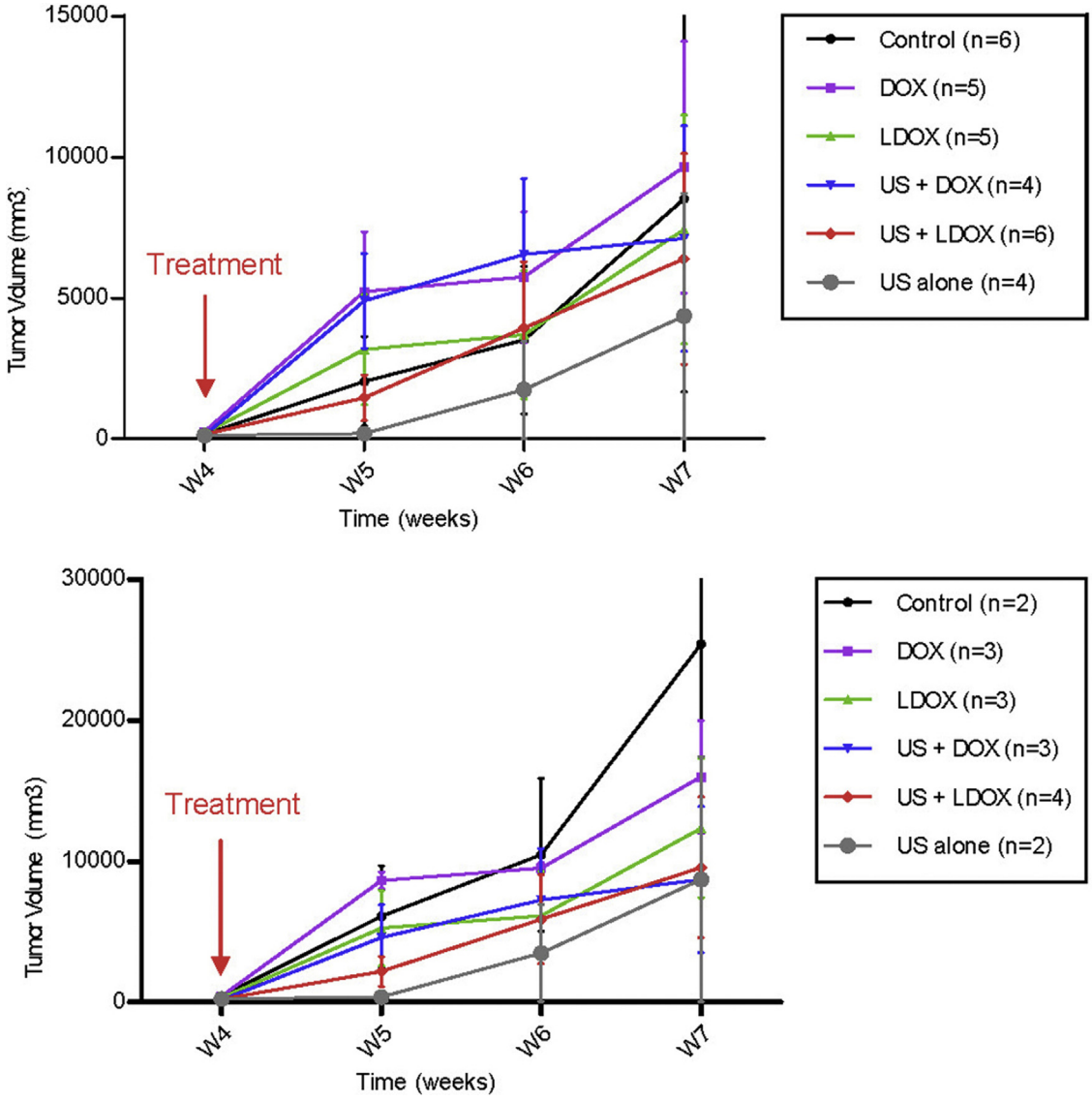

Figure 6 Tumors growth according to each treated group in orthotopic PDAC Lewis rat model. A. Considering all animals. B. Considering only animals with growing tumors > 80 mm^3 at 4 weeks.

pressures that collapse blood vessels in the tumor, leading to limited blood perfusion, insufficient drug delivery and absence of diffusion of MBUCA in the tumor [46]. In view of these considerations, obtaining cavitation without MBUCA can be considered highly desirable or even warranted for US triggered drug delivery to be efficient in PDAC.

We recognize that our study presents several limitations, the following three we wish to discuss briefly. The first is that positive results were not found significant in the rat model, and this was one reason for moving to the mouse model. As presented in the results section, the success rate of tumor implantation in Lewis rat model were not as high as reported by Hotz et al. in their original publication [24] and we found out that only tumors with a volume threshold of 80mm3 at 4 weeks could further growth, with a lower rate of spontaneous involution. Since only a fraction of the groups of rats had reached that threshold in our successive experiments, it turned out that restricting the analysis to those animals led to a trend in favour of better tumor control in the groups receiving ultrasound than chemotherapy alone, but due to the lack of power, that result did not reach statistical significance. The second limitation was our inability to show a significant advantage of US+L-DOX over a standard gemcitabine regimen in the mouse model. First, it must be noticed that although gemcitabine has a limited effect on patient survival in clinical studies, it is a powerful drug in animal models of PDAC [47]. It was therefore difficult to demonstrate a significant advantage of any new molecule or therapeutic combination over a standard gemcitabine regimen in the nude mouse model. Moreover, we had to select doxorubicin for liposomal experiments despite the poor efficacy of this drug on pancreatic tumor cells because methods for liposome encapsulation are well described with DOX and also because our consortium had the know-how to manufacture sonosensitive DOX-encapsulated liposomes, not GEM ones. A group of gemcitabine-based lipo-

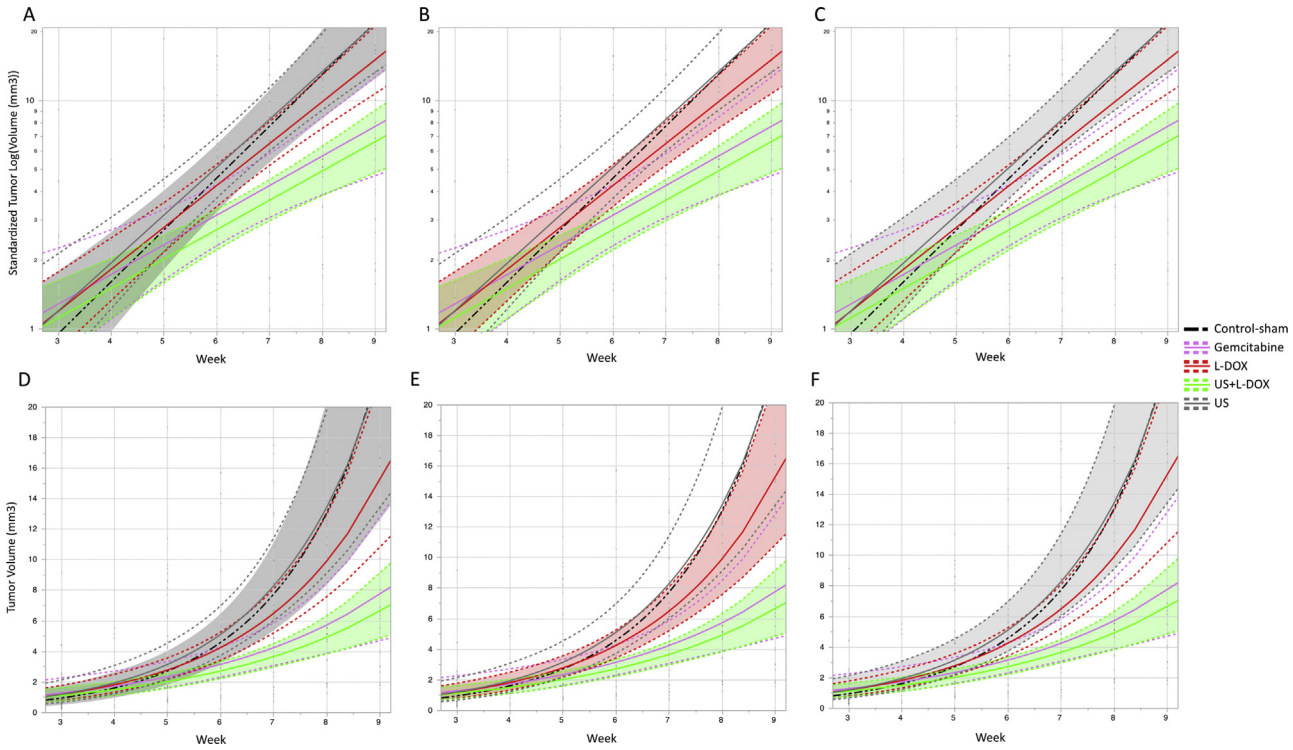

Figure 7 Tumors growth according to each treated group in in orthotopic PDAC nude mice. Results of the logistic regression on standardized Tumor Log (Volume (mm^3) with confidence intervals of each group (A, B, and C). Results of tumor volume growth with classical (non-log transformed) growth curves (D, E and F). Statistical significance was found between US+LDOX vs. either control, US and DOX groups. Confidence intervals highlighted for control vs. US+LDOX (A and D), LDOX vs. US+LDOX (B&E), and US vs. US + LDOX groups (C and F).

somes would have been desirable and might have yielded interesting results, but the lipophilic nature of gemcitabine makes it an uneasy candidate for encapsulation. Still, we found a trend, although non significant, for a slower growth rate under US + L-DOX than under gemcitabine, which in our view is already a very encouraging result. A third limitation was that a single treatment session was performed, which may limit the demonstration of efficacy. In a study on the efficacy of paclitaxel liposomes associated with systemic gemcitabine in an orthotopic xenograft model of pancreatic cancer in nude mice, [48] treatment was administered twice a week for 2 weeks. However, since our main objective in the efficacy study was the effect of US+liposomal drug on tumor growth, not on overall survival, a single session provided more readily interpretable data.

To our knowledge, there has been only one study on US therapy conducted in a genetically engineered model of PDAC (the KPC model) in the litterature with pulsed high intensity focused ultrasound (pHIFU) [49]. In this work, the authors demonstrated that pHIFU enhanced the concentration of the chemotherapeutic drug (Dox) in KPC mouse pancreatic tumors by up to 4.5-fold, possibly as a result of stromal matrix disruption. The study also demonstrated that passive drug diffusion through previously permeabilized tumor tissue was an important mechanism of drug delivery. However this study did not shown any efficacy data and the KPC model is not a perfect one for focused therapy since it induces multiple tumor foci which cannot be targeted separately. Nevertheless, implanted tumor models such as the Lewis rat and nude mouse used in this study are not perfect either since they lack one of the major components of tumor chemoresistance in PDAC, namely the stromal microenvironment.

Subsequently, we consider that before contemplating new animal studies, it would be warranted to implement our knowledge of:

- the mechanisms of liposome disruption (permeabilization by cavitation microjets, acoustically induced shear stress, bilayer seeded cavitation, or perhaps an entirely new mechanism which has yet to be fully described);
- the effects of cavitation on the tumor microenvironment and;
- the interaction of liposome and tumor stroma, to find out how liposomes can bypass the tumor matrix and release cytotoxic drugs only after matrix disruption.

The role of cavitation regimen (essentially stable or inertial, or a combination) is probably of paramount importance and its deciphering will require in vitro studies in 3D-models which are currently in progress in our group. Such models could help understand whether US and DOX (or LDOX) have additive or synergistic effect.

To conclude, this series of experiments confirmed the feasibility of combining Doxorubicin-loaded sonosensitive liposomes and focused ultrasonic cavitation to trigger local chemotherapy release in 2 different orthotopic murine models of PDAC. The present study also provides insights

into the pitfalls of cavitation-induced liposomal drug release and essential design considerations for further development of this technique. A deeper understanding of cavitation-induced mechanisms inducing cell permeation (sonoporation), but also stromal microenvironment disruption, is required.

Funding

This work was funded by ANR (agence nationale pour la recherche medicale), projet blanc, project named: USpDD.

Disclosure of interest

The authors declare that they have no competing interest.

Appendix A. Supplementary data

Supplementary material related to this article can be found, in the online version, at https://doi.org/10.1016/j.clinre.2019.02.015.

References

[1] Lucas AL, Malvezzi M, Carioli G, Negri E, La Vecchia C, Boffetta P, et al. Global Trends in Pancreatic Cancer Mortality From 1980 Through 2013 and Predictions for 2017. Clin Gastroenterol Hepatol 2016;14, http://dx.doi.org/10.1016/j.cgh.2016.05.034, 1452—1462.e4.

[2] Rahib L, Smith BD, Aizenberg R, Rosenzweig AB, Fleshman JM, Matrisian LM. Projecting cancer incidence and deaths to 2030: the unexpected burden of thyroid, liver, and pancreas cancers in the United States. Cancer Res 2014;74:2913—21, http://dx.doi.org/10.1158/0008-5472.CAN-14-0155.

[3] Siegel RL, Miller KD, Jemal A. Cancer statistics, 2018. CA Cancer J Clin 2018;68:7—30, http://dx.doi.org/10.3322/caac.21442.

[4] Conroy T, Hammel P, Hebbar M, Ben Abdelghani M, Wei AC, Raoul J-L, et al. Unicancer GI PRODIGE 24/CCTG PA.6 trial: A multicenter international randomized phase III trial of adjuvant mFOLFIRINOX versus gemcitabine (gem) in patients with resected pancreatic ductal adenocarcinomas. Journal of Clinical Oncology 2018;36, http://dx.doi.org/10.1200/JCO.2018.36.18_suppl.LBA4001. LBA4001—LBA4001.

[5] Neoptolemos JP, Palmer DH, Ghaneh P, Psarelli EE, Valle JW, Halloran CM, et al. Comparison of adjuvant gemcitabine and capecitabine with gemcitabine monotherapy in patients with resected pancreatic cancer (ESPAC-4): a multicentre, open-label, randomised, phase 3 trial. Lancet 2017;389:1011—24, http://dx.doi.org/10.1016/S0140-6736(16)32409-6.

[6] Sultana A, Tudur Smith C, Cunningham D, Starling N, Tait D, Neoptolemos JP, et al. Systematic review, including meta-analyses, on the management of locally advanced pancreatic cancer using radiation/combined modality therapy. Br J Cancer 2007;96:1183—90, http://dx.doi.org/10.1038/sj.bjc.6603719.

[7] Ducreux M, Cuhna AS, Caramella C, Hollebecque A, Burtin P, Goéré D, et al. Cancer of the pancreas: ESMO Clinical Practice Guidelines for diagnosis, treatment and follow-up. Ann Oncol 2015;26 Suppl 5, http://dx.doi.org/10.1093/annonc/mdv295, v56—68.

[8] Von Hoff DD, Ervin T, Arena FP, Chiorean EG, Infante J, Moore M, et al. Increased survival in pancreatic cancer with nab-paclitaxel plus gemcitabine. N Engl J Med 2013;369:1691—703, http://dx.doi.org/10.1056/NEJMoa1304369.

[9] Conroy T, Desseigne F, Ychou M, Bouché O, Guimbaud R, Bécouarn Y, et al. FOLFIRINOX versus gemcitabine for metastatic pancreatic cancer. N Engl J Med 2011;364:1817—25, http://dx.doi.org/10.1056/NEJMoa1011923.

[10] Neesse A, Michl P, Frese KK, Feig C, Cook N, Jacobetz MA, et al. Stromal biology and therapy in pancreatic cancer. Gut 2011;60:861—8, http://dx.doi.org/10.1136/gut.2010.226092.

[11] Vennin C, Murphy KJ, Morton JP, Cox TR, Pajic M, Timpson P. Reshaping the Tumor Stroma for Treatment of Pancreatic Cancer. Gastroenterology 2018;154:820—38, http://dx.doi.org/10.1053/j.gastro.2017.11.280.

[12] Böhmer MR, Klibanov AL, Tiemann K, Hall CS, Gruell H, Steinbach OC. Ultrasound triggered image-guided drug delivery. Eur J Radiol 2009;70:242—53, http://dx.doi.org/10.1016/j.ejrad.2009.01.051.

[13] Dimcevski G, Kotopoulis S, Bjånes T, Hoem D, Schjøtt J, Gjertsen BT, et al. A human clinical trial using ultrasound and microbubbles to enhance gemcitabine treatment of inoperable pancreatic cancer. J Control Release 2016;243:172—81, http://dx.doi.org/10.1016/j.jconrel.2016.10.007.

[14] Apfel RE, Holland CK. Gauging the likelihood of cavitation from short-pulse, low-duty cycle diagnostic ultrasound. Ultrasound Med Biol 1991;17:179—85.

[15] Ferrara K, Pollard R, Borden M. Ultrasound microbubble contrast agents: fundamentals and application to gene and drug delivery. Annu Rev Biomed Eng 2007;9:415—47, http://dx.doi.org/10.1146/annurev.bioeng.8.061505.095852.

[16] Hwang JH, Brayman AA, Reidy MA, Matula TJ, Kimmey MB, Crum LA. Vascular effects induced by combined 1-MHz ultrasound and microbubble contrast agent treatments in vivo. Ultrasound Med Biol 2005;31:553—64, http://dx.doi.org/10.1016/j.ultrasmedbio.2004.12.014.

[17] Poliachik SL, Chandler WL, Mourad PD, Bailey MR, Bloch S, Cleveland RO, et al. Effect of high-intensity focused ultrasound on whole blood with and without microbubble contrast agent. Ultrasound Med Biol 1999;25:991—8.

[18] Prieur F, Pillon A, Mestas J-L, Cartron V, Cèbe P, Chansard N, et al. Enhancement of Fluorescent Probe Penetration into Tumors In Vivo Using Unseeded Inertial Cavitation. Ultrasound Med Biol 2016;42:1706—13, http://dx.doi.org/10.1016/j.ultrasmedbio.2016.01.021.

[19] Lafond M, Mestas J-L, Prieur F, Chettab K, Geraci S, Clézardin P, et al. Unseeded Inertial Cavitation for Enhancing the Delivery of Chemotherapies: A Safety Study. Ultrasound Med Biol 2016;42:220—31, http://dx.doi.org/10.1016/j.ultrasmedbio.2015.08.019.

[20] Lafon C, Somaglino L, Bouchoux G, Mari JM, Chesnais S, Ngo J, et al. Feasibility study of cavitation-induced liposomal doxorubicin release in an AT2 Dunning rat tumor model 2012;20:691—702, http://dx.doi.org/10.3109/1061186X.2012.712129.

[21] Mestas J-L, Fowler RA, Evjen TJ, Somaglino L, Moussatov A, Ngo J, et al. Therapeutic efficacy of the combination of doxorubicin-loaded liposomes with inertial cavitation generated by confocal ultrasound in AT2 Dunning rat tumour model. J Drug Target 2014, http://dx.doi.org/10.3109/1061186X.2014.906604.

[22] Moussa HG, Martins AM, Husseini GA. Review on triggered liposomal drug delivery with a focus on ultrasound. Curr Cancer Drug Targets 2015;15:282—313.

[23] Journal officiel de la République française - N° 32 du 7 février 2013 - 13 09 arrete+agrément+établissments(2).pdf n.d.

[24] Hotz HG, Reber HA, Hotz B, Foitzik T, Buhr HJ, Cortina G, et al. An improved clinical model of orthotopic pancreatic cancer in immunocompetent Lewis rats. Pancreas 2001;22:113—21.

[25] Evjen TJ, Hagtvet E, Nilssen EA, Brandl M, Fossheim SL. Sonosensitive dioleoylphosphatidylethanolamine-containing liposomes with prolonged blood circulation time of doxorubicin. Eur J Pharm Sci 2011;43:318—24, http://dx.doi.org/10.1016/j.ejps.2011.05.007.
[26] Huwyler J, Drewe J, Krähenbuhl S. Tumor targeting using liposomal antineoplastic drugs. Int J Nanomedicine 2008;3:21—9.
[27] Evjen TJ, Nilssen EA, Rögnvaldsson S, Brandl M, Fossheim SL. Distearoylphosphatidylethanolamine-based liposomes for ultrasound-mediated drug delivery. Eur J Pharm Biopharm 2010;75:327—33, http://dx.doi.org/10.1016/j.ejpb.2010.04.012.
[28] Lafond M, Prieur F, Chavrier F, Mestas J-L, Lafon C. Numerical study of a confocal ultrasonic setup for cavitation creation. J Acoust Soc Am 2017;141:1935, http://dx.doi.org/10.1121/1.4978061.
[29] Kaiser AR, Cain CA, Hwang EY, Fowlkes JB, Jeffers RJ. A cost effective degassing system for use in ultrasonic measurements: The multiple pinhole degassing system. The Journal of the Acoustical Society of America 1996;99:3857—9, http://dx.doi.org/10.1121/1.415211.
[30] Lee MS, Dees EC, Wang AZ. Nanoparticle-Delivered Chemotherapy: Old Drugs in New Packages. Oncology (Williston Park NY) 2017;31:198—208.
[31] Drummond DC, Meyer O, Hong K, Kirpotin DB, Papahadjopoulos D. Optimizing liposomes for delivery of chemotherapeutic agents to solid tumors. Pharmacol Rev 1999;51:691—743.
[32] Lyseng-Williamson KA, Duggan ST, Keating GM. Pegylated liposomal doxorubicin: a guide to its use in various malignancies. BioDrugs 2013;27:533—40, http://dx.doi.org/10.1007/s40259-013-0070-1.
[33] Fowler RA, Fossheim SL, Mestas J-L, Ngo J, Canet-Soulas E, Lafon C. Non-invasive magnetic resonance imaging follow-up of sono-sensitive liposome tumor delivery and controlled release after high-intensity focused ultrasound. Ultrasound Med Biol 2013;39:2342—50, http://dx.doi.org/10.1016/j.ultrasmedbio.2013.06.002.
[34] Tove J, Evjen E, Hagtvet A, Moussatov S, Røgnvaldsson J-L, Mestas R, Andrew Fowler, et al. In vivo monitoring of liposomal release in tumours following ultrasound stimulation. 2013;84:526—31, http://dx.doi.org/10.1016/j.ejpb.2012.12.007.
[35] Qin J, Wang T-Y, Willmann JK. Sonoporation: Applications for Cancer Therapy. Adv Exp Med Biol 2016;880:263—91, http://dx.doi.org/10.1007/978-3-319-22536-4_15.
[36] Derieppe M, Rojek K, Escoffre J-M, de Senneville BD, Moonen C, Bos C. Recruitment of endocytosis in sonopermeabilization-mediated drug delivery: a real-time study. Phys Biol 2015;12:046010, http://dx.doi.org/10.1088/1478-3975/12/4/046010.
[37] Lentacker I, Geers B, Demeester J, De Smedt SC, Sanders NN. Design and evaluation of doxorubicin-containing microbubbles for ultrasound-triggered doxorubicin delivery: cytotoxicity and mechanisms involved. Mol Ther 2010;18:101—8, http://dx.doi.org/10.1038/mt.2009.160.
[38] van Wamel A, Sontum PC, Healey A, Kvåle S, Bush N, Bamber J, et al. Acoustic Cluster Therapy (ACT) enhances the therapeutic efficacy of paclitaxel and Abraxane® for treatment of human prostate adenocarcinoma in mice. J Control Release 2016;236:15—21, http://dx.doi.org/10.1016/j.jconrel.2016.06.018.
[39] Lammertink BHA, Bos C, van der Wurff-Jacobs KM, Storm G, Moonen CT, Deckers R. Increase of intracellular cisplatin levels and radiosensitization by ultrasound in combination with microbubbles. J Control Release 2016;238:157—65, http://dx.doi.org/10.1016/j.jconrel.2016.07.049.
[40] Theek B, Baues M, Ojha T, Möckel D, Veettil SK, Steitz J, et al. Sonoporation enhances liposome accumulation and penetration in tumors with low EPR. J Control Release 2016;231:77—85, http://dx.doi.org/10.1016/j.jconrel.2016.02.021.
[41] Carpentier A, Canney M, Vignot A, Reina V, Beccaria K, Horodyckid C, et al. Clinical trial of blood-brain barrier disruption by pulsed ultrasound. Sci Transl Med 2016;8, http://dx.doi.org/10.1126/scitranslmed.aaf6086, 343re2.
[42] Chettab K, Roux S, Mathé D, Cros-Perrial E, Lafond M, Lafon C, et al. Spatial and Temporal Control of Cavitation Allows High In Vitro Transfection Efficiency in the Absence of Transfection Reagents or Contrast Agents. PLoS ONE 2015;10, http://dx.doi.org/10.1371/journal.pone.0134247, e0134247.
[43] Fowlkes JB, Crum LA. Cavitation threshold measurements for microsecond length pulses of ultrasound. J Acoust Soc Am 1988;83:2190—201.
[44] Erkan M, Hausmann S, Michalski CW, Fingerle AA, Dobritz M, Kleeff J, et al. The role of stroma in pancreatic cancer: diagnostic and therapeutic implications. Nat Rev Gastroenterol Hepatol 2012;9:454—67, http://dx.doi.org/10.1038/nrgastro.2012.115.
[45] Jacobetz MA, Chan DS, Neesse A, Bapiro TE, Cook N, Frese KK, et al. Hyaluronan impairs vascular function and drug delivery in a mouse model of pancreatic cancer. Gut 2013;62:112—20, http://dx.doi.org/10.1136/gutjnl-2012-302529.
[46] Jain RK. An indirect way to tame cancer. Sci Am 2014;310:46—53.
[47] Awasthi N, Zhang C, Schwarz AM, Hinz S, Wang C, Williams NS, et al. Comparative benefits of Nab-paclitaxel over gemcitabine or polysorbate-based docetaxel in experimental pancreatic cancer. Carcinogenesis 2013;34:2361—9, http://dx.doi.org/10.1093/carcin/bgt227.
[48] Mao Y, Li X, Chen G, Wang S. Thermosensitive Hydrogel System With Paclitaxel Liposomes Used in Localized Drug Delivery System for In Situ Treatment of Tumor: Better Antitumor Efficacy and Lower Toxicity. J Pharm Sci 2016;105:194—204, http://dx.doi.org/10.1002/jps.24693.
[49] Li T, Wang Y-N, Khokhlova TD, D'Andrea S, Starr F, Chen H, et al. Pulsed High-Intensity Focused Ultrasound Enhances Delivery of Doxorubicin in a Preclinical Model of Pancreatic Cancer. Cancer Res 2015;75:3738—46, http://dx.doi.org/10.1158/0008-5472.CAN-15-0296.